Biosensors and Bioelectronics 124–125 (2019) 216–223

Contents lists available at ScienceDirect

Biosensors and Bioelectronics

journal homepage: www.elsevier.com/locate/bios

Development of a third-generation glucose sensor based on the open circuit potential for continuous glucose monitoring

Inyoung Lee[a,b], Noya Loew[b], Wakako Tsugawa[a], Kazunori Ikebukuro[a], Koji Sode[a,b,*]

[a] Department of Biotechnology and Life Science, Graduate School of Engineering, Tokyo University of Agriculture and Technology, 2-24-16 Naka-cho, Koganei, Tokyo 184-8588, Japan

[b] Joint Department of Biomedical Engineering, University of North Carolina at Chapel Hill, Chapel Hill, North Carolina 27599 and North Carolina State University, Raleigh, NC 27695, USA

ARTICLE INFO

Keywords:
Open circuit potential
Third generation glucose sensor
Continuous glucose monitoring (CGM)
Direct electron transfer
FAD dependent glucose dehydrogenase (FADGDH)

ABSTRACT

Continuous glucose monitoring (CGM) systems are most important in the current Type I diabetes care and as component for the development of artificial pancreas systems because the amount of insulin being supplied is calculated based on the CGM results. Therefore, to stably and accurately control the blood glucose level, CGM should be stable and accurate for a long period. We have been engaged in the biomolecular engineering and application of FAD dependent glucose dehydrogenase complex (FADGDH) which is capable of direct electron transfer. In this study, we report the development of the third-generation type open circuit potential (OCP) principle-based glucose sensor with direct electron transfer FADGDH immobilized on gold electrodes using a self-assembled monolayer (SAM). We developed a novel algorithm for OCP-based glucose sensors. By employing this new algorithm, high reproducibility of measurement and sensor preparation were achieved. In addition, the signal was not affected by the presence of acetaminophen and ascorbic acid in the sample solution. The thus optimized third-generation OCP-based glucose sensor could be operated continuously for more than 9 days without significant change in the signal, sensitivity and dynamic range, indicating its potential application for CGM systems.

1. Introduction

To control the blood glucose level of Type I diabetes patients, it should be required to continuously monitor the blood glucose concentration and supply insulin based on the measured glycemic level in the body. Recently, the U.S. Food and Drug Administration (FDA) approved a medical device comprising a continuous glucose monitoring (CGM) system, a continuous subcutaneous insulin infusion pump and a control algorithm that can supply an appropriate amount of basal insulin based on the CGM results as an artificial pancreas. Consequently, it became possible to automatically and continuously control the blood glucose level.

CGM is the most important component in the artificial pancreas system because the amount of insulin being supplied is calculated based on the CGM results. The incorrect amount of insulin infusion due to incorrect CGM results makes diabetes patients hypoglycemic, and, in the worst case, may result in death. To stably and accurately control the blood glucose level, CGM should be stable and accurate for a long period. Therefore, many researchers have tried to improve the stability and accuracy of CGM sensors (Rodbard et al., 2016; I. Lee et al., 2018; H. Lee et al., 2018). Among CGM sensors, those based on the electrochemical principle comprising an enzyme reaction, particularly the amperometric principle, are used widely and are already commercially available because of their high sensitivity and simplicity.

Among the amperometric principle-based CGM sensors, electrochemical-based CGM sensors can be historically divided into 3 generations of CGM sensors according to the electron acceptor and characteristic of the oxidative half-reaction. In the first-generation enzyme sensor that utilizes glucose oxidase (GOx), the enzyme oxidizes glucose to gluconolactone while its cofactor FAD is reduced, and the reduced FAD transfers electrons to oxygen to form hydrogen peroxide. Finally, the electrochemical signal can be detected by either measuring decreased concentration of oxygen or the liberated hydrogen peroxide. However, the sensor signal of first-generation enzyme sensors is easily affected by interfering substances because a high potential should be applied to monitor oxygen or hydrogen peroxide. Additionally, the sensor signal is affected by the dissolved oxygen concentration of the sample because GOx uses oxygen as the primary electron acceptor. In the second-generation enzyme sensor that utilizes either GOx or glucose

* Corresponding author at: Joint Department of Biomedical Engineering, University of North Carolina at Chapel Hill, Chapel Hill, North Carolina 27599 and North Carolina State University, Raleigh, NC 27695, USA.
E-mail address: ksode@email.unc.edu (K. Sode).

https://doi.org/10.1016/j.bios.2018.09.099
Received 30 June 2018; Received in revised form 10 September 2018; Accepted 29 September 2018
Available online 09 October 2018
0956-5663/

dehydrogenases, artificial electron acceptors (mediators) are used instead of oxygen. The reduced FAD formed by the oxidation of glucose transfers electrons to the mediators. The electrochemical signal can be detected by oxidizing the reduced mediators. The second-generation CGM sensor has the advantage that the sensor signal is obtained without being affected by the oxygen concentration. However, problems persist such as the effect of interfering substances by the mediator and potential application. For reducing the effect of interfering substances in first and second generation CGM sensor, it is important that the electrode potential should be lowered enough to prevent oxidation of interfering substances on the electrode surface. To lower the applied potential, several mediators have been investigated which led to the development of the historical achievement of Osmium polymer type mediator (Ohara et al., 1994). Conventionally, an ion-selective membrane, such as Nafion, is employed to prevent access of interfering substances (Moatti-Sirat et al., 1994). However, the development of further simplified methods/technologies to prepare sensors that are unaffected by ingredients are still in a great demand. On the other hand, in the third-generation CGM sensor that utilizes a direct electron transfer-type enzyme, the enzyme can transfer electrons to the electrode directly without any electron acceptor; therefore, the sensor signal is not affected by oxygen or mediator. Because of its simple electron transfer pathway, third-generation CGM sensors are expected to be a highly accurate and stable CGM sensors that can resolve the problems of the first- and second-generation CGM sensors.

Previously, we reported of a glucose dehydrogenase capable of direct electron transfer: the FAD-dependent glucose dehydrogenase complex (FADGDH) derived from *Burkholderia cepacia* (Sode et al., 1996; Yamazaki et al., 1999; Inose et al., 2003; Yamaoka et al., 2004; Tsuya et al., 2006). This enzyme complex consists of 3 subunits; a catalytic subunit, a small subunit and an electron transfer subunit. Glucose is oxidized by the catalytic subunit of this enzyme, and electrons generated by the oxidation of glucose are transferred to the electron transfer subunit via intramolecular electron transfer (FAD, 3Fe-4S cluster and hemes) (Shiota et al., 2016; Yamashita et al., 2018). Finally, the electron is transferred to the electrode by the heme of the electron transfer subunit. Owing to this direct electron transfer ability of FADGDH, the enzyme is expected to be a sensor element of the third-generation CGM sensor that can prevent the effect of the oxygen and mediator. We have already reported several electrochemical principles based on third-generation glucose sensors utilizing direct electron transfer FADGDH. We reported a self-powered glucose sensing system employing our original concept, the BioCapacitor principle, which consists of an enzyme fuel cell, a charge pump and a capacitor, and we succeeded in measuring the glucose concentration autonomously based on this principle (Hanashi et al., 2009, 2011, 2012; Sode et al., 2016). In addition, we reported of the operation of a stepping motor (Hanashi et al., 2014) and a microcontroller (Lee et al., 2017) based on this BioCapacitor principle. Recently, we also reported of the development of an amperometric glucose sensor combining direct electron transfer FADGDH and a self-assembled monolayer (SAM) (I. Lee et al., 2018). This sensor could measure the glucose concentration without any other electron acceptor. Additionally, the potential applied in the amperometric measurement could be lowered by employing FADGDH, which has a lower redox potential than most mediators, and we could prevent the effect of interfering substances on the sensor signal.

Open circuit potential (OCP) is the potential of an electrode in the open circuit state. When the circuit is opened, current cannot flow in the circuit; therefore, there is no current. Glucose sensors based on the measurement of OCP have been reported, and were also divided into 3 generations. (Song et al., 2017; Katz et al., 2001). However, the first- and second-generation OCP-based glucose sensors cannot avoid the problems of which the first- and second-generation amperometric glucose sensor are suffering. On the other hand, the third-generation OCP glucose sensor is expected to measure the glucose concentration stably without any other electron acceptor, indicating the possibility of its application as a high-performance CGM sensor. We previously reported of a study on a third generation type enzyme fuel cell type glucose sensor using direct electron transfer FADGDH (Kakehi et al., 2007), where we monitored the open circuit voltage of an enzyme fuel cell. However, some challenges remained for a successful application for CGM. First, the former sensor employed an enzyme fuel cell type configuration including a platinum cathode, which turned out to be not necessary for the construction of an OCP type sensor. Furthermore, the operational protocol had yet to be established. The characterization of the repeatability and reproducibility of the sensor, the effect of interfering substances, and the long term operation, is also required in order to use third-generation OCP-based glucose sensors for future CGM sensors.

Focusing on the current urgent expected superior characteristic of third generation type sensor, we revive the OCP principle-based glucose sensor with direct electron transfer FADGDH. The third-generation type OCP principle-based glucose sensor was developed with direct electron transfer FADGDH immobilized on gold electrode by SAM. By the employment of a new algorithm, high reproducibility of the measurements and the sensor preparation were achieved. In addition, the signal was not affected by the presence of acetaminophen and ascorbic acid in the sample solution. The thus optimized third-generation OCP-based glucose sensor could be operated continuously for more than 9 days without significant change in the signal, sensitivity and dynamic range, indicating its potential application for CGM system.

2. Materials and methods

2.1. Chemicals and materials

In this study, the bacterial FAD-dependent glucose dehydrogenase complex (FADGDH) was used. The direct electron transfer FADGDH comprises three subunits: the catalytic subunit, heme *c* containing electron transfer subunit, and small subunit. A recombinant FADGDH was prepared using the expression vectors pTrc99A containing the structural gene for the FADGDH and pAYCYC184 containing the structural genes for heme *c* maturation (pEC86). The vectors were transformed into *Escherichia coli* strain BL21 (DE3) and cultivated as previously described (Tsuya et al., 2006). Dithiobis(succinimidyl hexanoate) (DSH) was purchased from Dojindo Molecular Technologies, Inc. (Kumamoto, Japan). Gold disk electrode (GDE), platinum (Pt) wire and a silver/silver chloride (Ag/AgCl) reference electrode were purchased from BAS Inc. (Tokyo, Japan). Acetone and D (+)-Glucose were purchased from Wako Pure Chemical Industries, Ltd. (Osaka, Japan). L(+)-Ascorbic Acid was purchased from Sigma-Aldrich (St. Louis, MO, USA) and 4′-hydroxyacetanilide (acetaminophen) was purchased from Tokyo Chemical Industry Co., Ltd. (Tokyo, Japan).

2.2. Preparation of GDE with SAM immobilized direct electron transfer FADGDH

GDEs (Electrode surface area: 7 mm^2) were washed using piranha solution and acetone. To construct SAM-modified electrodes, washed GDEs were incubated in 200 µl of 10 µM DSH solution overnight at 25 °C, as was described previously (I. Lee et al., 2018). The SAM-modified GDEs were then washed with acetone and incubated in 1 ml of enzyme solution, including 0.014 mg/ml of direct electron transfer FADGDH solution overnight at 25 °C. The completed enzyme electrodes were stored in 100 mM potassium phosphate buffer (pH 7.0) until use.

2.3. Glucose measurement with the OCP-based glucose sensor employing a novel measurement algorithm

The constructed direct electron transfer enzyme electrode (working electrode) was evaluated using a 10-ml water-jacket cell, with the Ag/AgCl and Pt wire as the reference electrode and counter electrode. A potentiostat measured OCP continuously between the constructed direct electron transfer enzyme electrode and Ag/AgCl. Additionally, the other potentiostat applied + 100 mV (vs. Ag/AgCl) for 10 s before every OCP data sampling. Using 3 constructed enzyme electrodes, we compared the

repeatability and reproducibility of the enzyme electrodes between conventional measurement and a novel measurement algorithm. First, in the evaluation of repeatability, we carried out calibrations on each electrode 3 times. Additionally, in the evaluation of reproducibility, we compared the calibrations of 3 enzyme electrodes.

2.4. Investigation of the effect of interfering substances on the sensor signal of OCP based on the third-generation glucose sensor employing a novel measurement algorithm

The constructed direct electron transfer enzyme electrode (working electrode) was evaluated using a 10-ml water jacket cell in the absence/presence of 170 μM ascorbic acid or 1.3 mM acetaminophen, with Ag/AgCl and Pt wire as the reference electrode and counter electrode, respectively. The one potentiostat measured OCP between the constructed direct electron transfer enzyme electrode and Ag/AgCl continuously and recorded the potential every second. The second potentiostat was utilized for the potential application to enzyme electrode (+ 100 mV vs. Ag/AgCl) for 10 s when the steady state potential was observed. After this potential application, the second potentiostat remained disconnected, and the steady state potential was recorded as the measure of the corresponding glucose concentration in the solution.

2.5. Continuous measurement of OCP based on a third-generation glucose sensor employing a novel measurement algorithm

The constructed direct electron transfer enzyme electrode (working electrode) was evaluated using a 10-ml water-jacket cell in the presence of 20 mM glucose, with the Ag/AgCl and Pt wire as the reference electrode and counter electrode, respectively. According to the developed algorithm of the measurement, the first potentiostat measured OCP between the constructed direct electron transfer enzyme electrode and Ag/AgCl continuously and recorded the potential every second. The second potentiostat was programmed to apply potential to enzyme electrode (+ 100 mV vs. Ag/AgCl) for 10 s with the 5 min interval, repeatedly. After 5 min of this potential application, the steady state potential was recorded by the first potentiostat as the measure of the corresponding glucose concentration in the solution.

3. Results and discussion

3.1. Development of the OCP-based glucose sensor employing a novel measurement algorithm

We previously reported of an OCP sensor employing an enzyme fuel cell, which was composed of a carbon paste anode with direct electron transfer type FADGDH immobilized using glutaraldehyde as cross-linker, and a Pt cathode. However, a cathode is not necessary for OCP measurements, and therefore, in this study, we employed a much simpler configuration for the OCP sensor, using a gold electrode with direct electron transfer type FADGDH, immobilized by SAM, for which we have demonstrated clearly that direct electron transfer between the gold electrode and the enzyme occurs (I. Lee et al., 2018). Addition of glucose clearly resulted the decrease of OCP when this direct electron

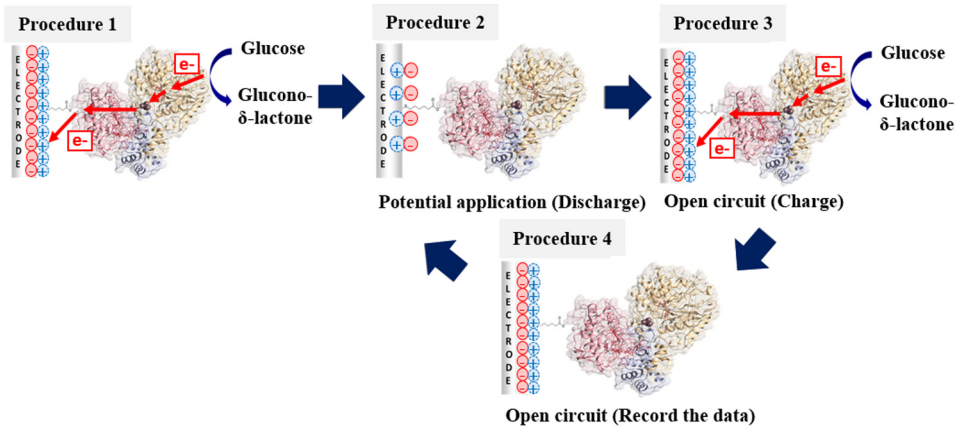

Scheme 1. Schematic of a novel OCP measurement algorithm The novel OCP measurement algorithm consists of 4 steps: Procedure 1: Direct electron transfer of FADGDH charges electrons to the electrode surface in the presence of glucose. Procedure 2: Charged electrons are discharged by applying a potential (+ 100 mV (vs. Ag/AgCl)) to the enzyme electrode for 10 s. Procedure 3: The electrode state is returned to open circuit, and the enzyme again charges electrons to the electrode surface. Procedure 4: When OCP becomes stable, the OCP is recorded.

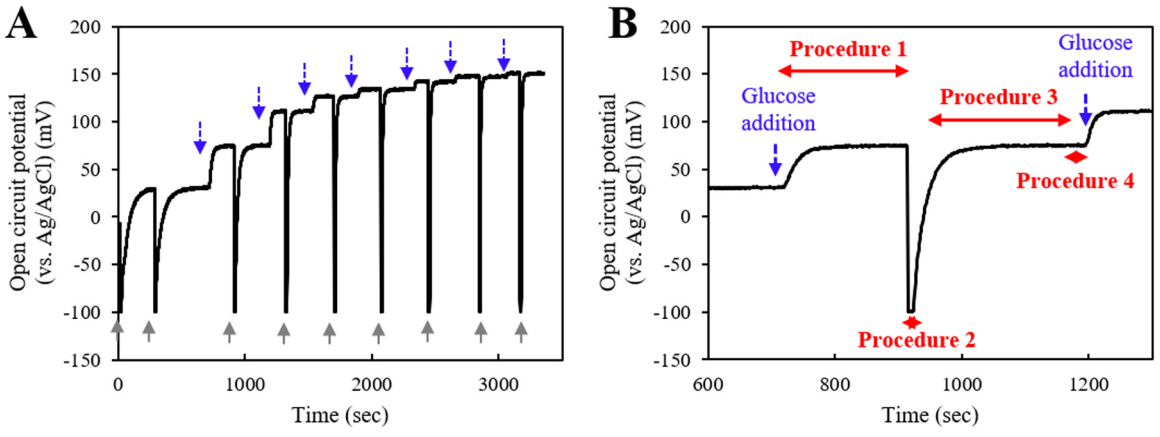

Fig. 1. Electrochemical evaluations of the OCP change between the direct electron transfer FADGDH electrode employing a novel OCP measurement algorithm (A) OCP evaluation of the direct electron transfer FADGDH immobilized electrode in 100 mM potassium phosphate buffer (pH 7.0), followed by the addition of 0.1, 1, 3, 5, 10, 15, and 20 mM glucose at the dashed arrows and + 100 mV (vs. Ag/AgCl) potential application at the solid arrows. (B) Enlarged Fig. 1 (A). Procedure 1–4 refer to the novel OCP measurement algorithm described in Scheme 1.

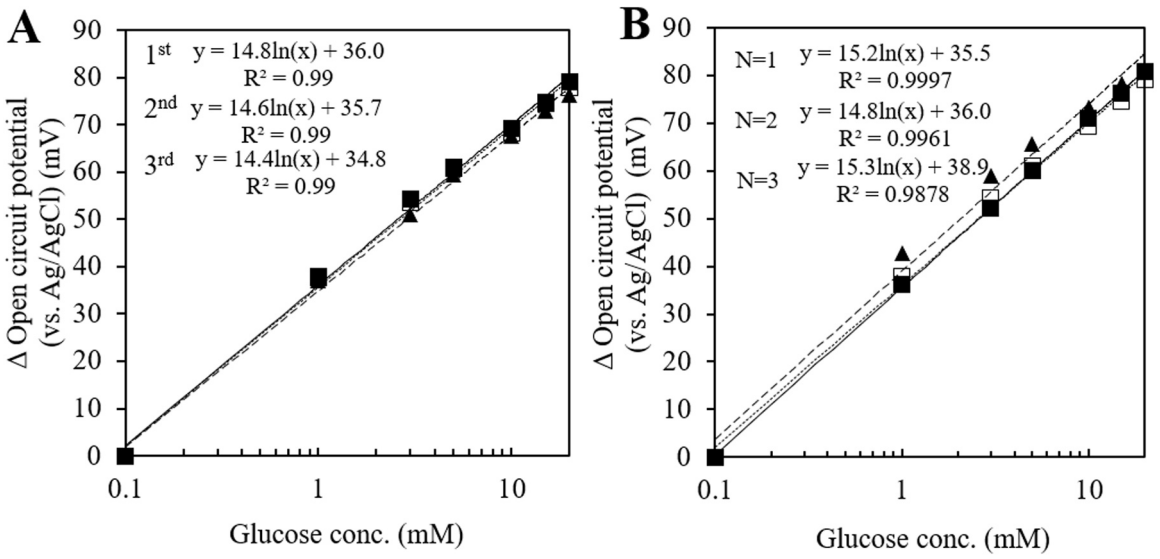

Fig. 2. The repeatability (Fig. 2A) and reproducibility (Fig. 2B) of the measurement and electrode preparation of the OCP-based glucose sensor between the novel OCP measurement algorithm and the conventional measurement We calculated the ΔOCP as difference between the OCP value at each glucose concentration and the OCP value in presence of 0.1 mM glucose. (A) Three representative calibration curves using the same electrode. Evaluation of the direct electron transfer FADGDH immobilized electrode in 100 mM potassium phosphate buffer (pH 7.0). Before each OCP data sampling, + 100 mV (vs. Ag/AgCl) was applied to the OCP-based glucose sensor for 10 s. Filled squares and solid line show the calibration curve of the first measurement (1st), open squares and dotted line show the calibration curve of the second measurement (2nd), and filled triangles and dashed line show the calibration of the third measurement (3rd). Evaluations were carried out in triplicate. We reversed the sign of the potential to ease the interpretation. (B) Representative calibration curves using three different electrodes. Evaluation of the direct electron transfer FADGDH immobilized electrode in 100 mM potassium phosphate buffer (pH 7.0). Before each OCP data sampling, + 100 mV (vs. Ag/AgCl) was applied to the OCP-based glucose sensor for 10 s. Filled squares and solid line show the calibration curve of the first electrode (N = 1), open squares and dotted line show the calibration curve of the second electrode (N = 2), and filled triangles and dashed line show the calibration curve of the third electrode (N = 3). Evaluations were carried out in triplicate. We reversed the sign of the potential to ease the interpretation.

Table 1
The comparison of standard deviation of repeatability and reproducibility between conventional measurement and a novel OCP measurement algorithm. Evaluations were carried out in triplicate (N = 3).

(N = 3)	Conventional measurement	A novel OCP measurement algorithm
Repeatability of 3 times measurement using same electrode	0.5	0.2
Reproducibility of the 3 electrode preparations	1.0	0.2

transfer type FADGDH electrode was used. In contrast, when a corresponding electrode with non-direct electron transfer type fungi derived FADGDH (Mori et al., 2011) was used, no OCP decrease due to glucose was observed (Supplementary information S1-A and B), confirming that the observed OCP change was due to the 3rd generation type enzyme.

In the open circuit state, once electrons are charged on the electrode surface, they remain on the electrode surface because there is no current flow. We considered that these remaining electrons are the reason for the low repeatability and reproducibility. Thus, to obtain an accurate glucose concentration-dependent OCP change with every measurement, it is necessary to reset the electrical state of the electrode surface to the same state before every measurement. In other words, it is necessary to discharge charged electrons before measurement. A successful discharge can be achieved by applying a potential that is sufficiently high to oxidize the reduced enzyme. In our previous study, reduced direct electron transfer type FADGDH was efficiently oxidized by applying + 100 mV (vs. Ag/AgCl) (I. Lee et al., 2018). In this study, we investigated the application of potentials above + 100 mV (vs. Ag/AgCl) (+100, +200, +300 and +400 mV (vs. Ag/AgCl)) for 0.1, 1, 10 or 60 s for discharging and resetting the electrode surface. We did not observe any significant difference due to the applied potential. However, the duration of potential application affected the sensitivity of the sensor (slope). The observed slopes increased with increasing duration of potential application, up to 10 s of potential application, but no significant increase of the slope was observed by applying a potential for 60 s (Supplementary information S2). Considering that application of a higher potential might cause unnecessary turnover of catalytic reaction, and consequently may cause inactivation of the enzyme, we employed the conditions of a potential application for 10 s at + 100 mV vs Ag/AgCl.

Scheme 1 shows a novel OCP measurement algorithm that carries out discharging of charged electrons before every measurement. In the initial stage, glucose in the solution is oxidized by FADGDH in its catalytic reaction and the reduced direct electron transfer FADGDH charges electrons to the electrode surface (Procedure 1). Next, the charged electrons are discharged by applying a potential (+ 100 mV vs. Ag/AgCl) to the enzyme electrode for 10 s (Procedure 2). The electrical state of the enzyme electrode surface can be reset by this procedure. Then, the electrode state is returned to open circuit and the enzyme again charges electrons to the electrode surface in the presence of glucose (Procedure 3). Finally, when the OCP becomes stable, OCP is recorded (Procedure 4), and the potential is applied to the electrode again for the next measurement (Procedure 2).

Fig. 1 shows the time course of the continuous measurement of glucose by sequential addition of glucose sample to the solution with the above-mentioned novel algorithm. Fig. 1B shows the enlarged time course between 600 s and 1300 s. At around 600 s, glucose sample was

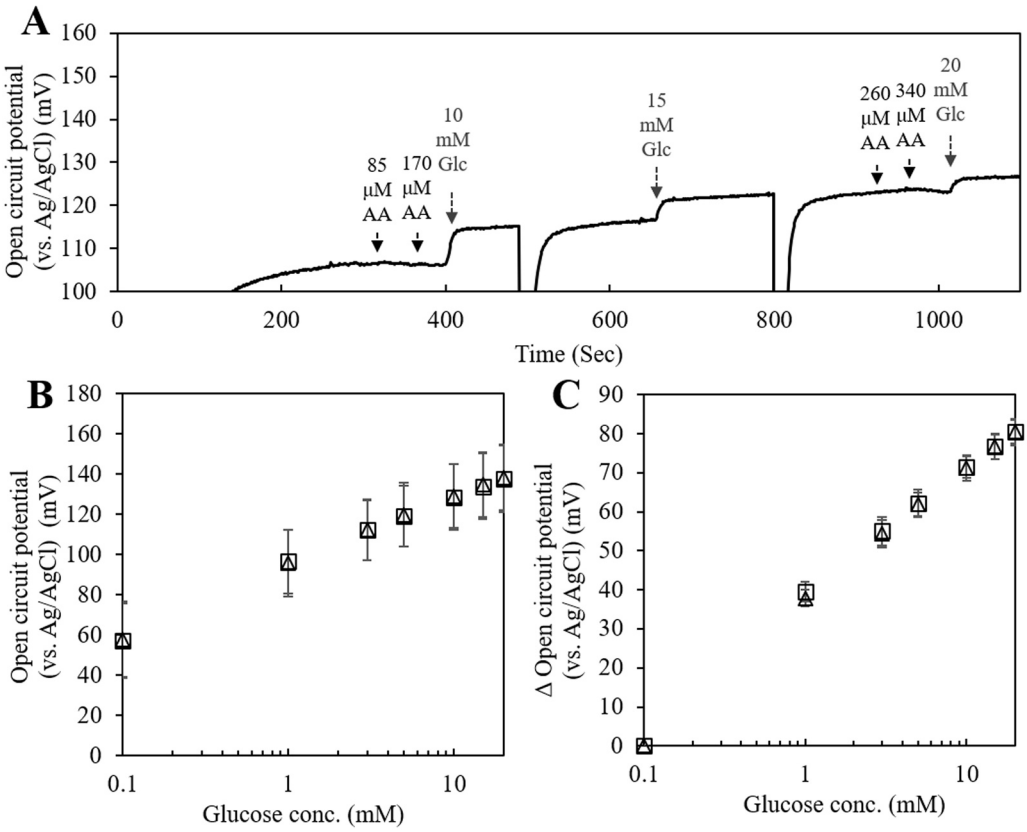

Fig. 3. Investigation of the effect of ascorbic acid on the sensor signal of OCP-based third-generation glucose sensor employing a novel measurement algorithm. (A) Representative time course. OCP evaluation of the direct electron transfer FADGDH immobilized electrode in 100 mM potassium phosphate buffer (pH 7.0). Before each OCP data sampling, + 100 mV (vs. Ag/AgCl) was applied to the OCP-based glucose sensor for 10 s. Additionally, we added 85, 170, 260, 340 μM ascorbic acid (AA) and 10, 15, 20 mM glucose at the dashed arrows. We reversed the sign of the potential to ease the interpretation. (B) Comparison of the OCP calibration curve in the absence or presence of 170 μM ascorbic acid. OCP evaluation of the direct electron transfer FADGDH immobilized electrode in 100 mM potassium phosphate buffer (pH 7.0) in the absence or presence of 170 μM ascorbic acid. Before each OCP data sampling, + 100 mV (vs. Ag/AgCl) was applied to the OCP-based glucose sensor for 10 s. Open squares show the calibration curve in the absence of ascorbic acid, and open triangles show the calibration curve in the presence of 170 μM ascorbic acid. Evaluations were carried out in triplicate, and error bars indicate the respective standard deviations. We reversed the sign of the potential to ease the interpretation. (C) Comparison of the ΔOCP calibration curve in the absence or presence of 170 μM ascorbic acid. We calculated the ΔOCP as difference of the OCP value at each glucose concentration to the OCP value in presence of 0.1 mM glucose. ΔOCP evaluation of the direct electron transfer FADGDH immobilized electrode in 100 mM potassium phosphate buffer (pH 7.0) in the absence or presence of 170 μM ascorbic acid. Before each OCP data sampling, + 100 mV (vs. Ag/AgCl) was applied to the OCP-based glucose sensor for 10 s. Open squares show the calibration curve in the absence of ascorbic acid, and open triangles show the calibration curve in the presence of 170 μM ascorbic acid. Evaluations were carried out in triplicate, and error bars indicate the respective standard deviation. We reversed the sign of the potential to ease the interpretation.

added and resulted in an increase of the OCP (Procedure 1). After the steady state potential was observed, + 100 mV vs. Ag/AgCl was applied to the enzyme electrode for 10 s (Procedure 2). After this procedure, the potential recovered to its steady state potential (Procedure 3), then the potential was recorded (Procedure 4) as the potential at this glucose concentration.

We compared the reproducibility of the measurement and electrode preparation of the OCP-based glucose sensor between the novel OCP measurement algorithm and the conventional measurement which we used as standard. Fig. 2A shows the repeatability of the measurement using the same electrode for the OCP-based glucose sensor. By employing the novel OCP measurement algorithm, high repeatability was achieved. In contrast to this, when the same measurement was carried out for 3 times using the same electrode and under the same conditions, but with conventional procedure for measurement, all the slopes of the calibration curves were greatly different (Supplementary information S3A). Similarly, Fig. 2B shows the reproducibility of the 3 electrode preparations. By employing the novel OCP measurement algorithm, high reproducibility was achieved compared to employing the conventional method (Supplementary information S3B). Table 1 summarizes these results showing the standard deviations of the slopes of the obtained calibration curves. By employing our novel OCP measurement algorithm, a lower standard deviation was achieved in both reproducibility of the measurement and of the electrode preparation compared with conventional measurements. Considering the linearity of the sensor calibration, three calibration curves with three different dynamic ranges were provided (Supplementary information S4). Among them, the one which covers glucose concentration from 0.5 mM to 50 mM was fully satisfactory to monitor the physiologically relevant glucose concentration range, including hypoglycemia, which is below 70 mg/dl (approximately 3.9 mM), and hyperglycemia, which is above 180 mg/dl (approximately 10 mM). The limit of detection was estimated to be 0.1 mM (Supplementary information S4). Current commercially available CGM sensors can detect from 40 mg/dl (2.2 mM) to 400 mg/dl (22 mM), therefore, this OCP based sensor can provide a sufficient or an even wider dynamic range for CGM application. The additional two calibrations covering glucose concentration of 0.001–0.5 mM, or of 50–200 mM, might lead to other potential applications of this continuous real time glucose sensing system.

3.2. Investigation of the effect of interfering substances on the sensor signal of OCP based on the third-generation glucose sensor employing a novel measurement algorithm

We investigated the effect of ascorbic acid and acetaminophen on the sensor signal of OCP based on the third-generation glucose sensor employing a novel OCP measurement algorithm. First, we investigated the effect of ascorbic acid. Fig. 3A shows the time course, and we investigated the OCP change by adding ascorbic acid and glucose into the reaction buffer. When ascorbic acid was added, there was no significant change in the OCP. On the other hand, when glucose was added, the OCP was clearly changed. Furthermore, even when 340 μM ascorbic acid (2 times higher than the FDA-recommended concentration) was added to evaluate the glucose sensor, there was no effect of ascorbic acid. Fig. 3B and C shows calibration curves and the slopes of calibration curves (ΔOCP) with or without 170 μM ascorbic acid. Both the OCP and slope of the calibration curve were not affected by ascorbic acid. Similarly, we investigated the effect of acetaminophen. The FDA has

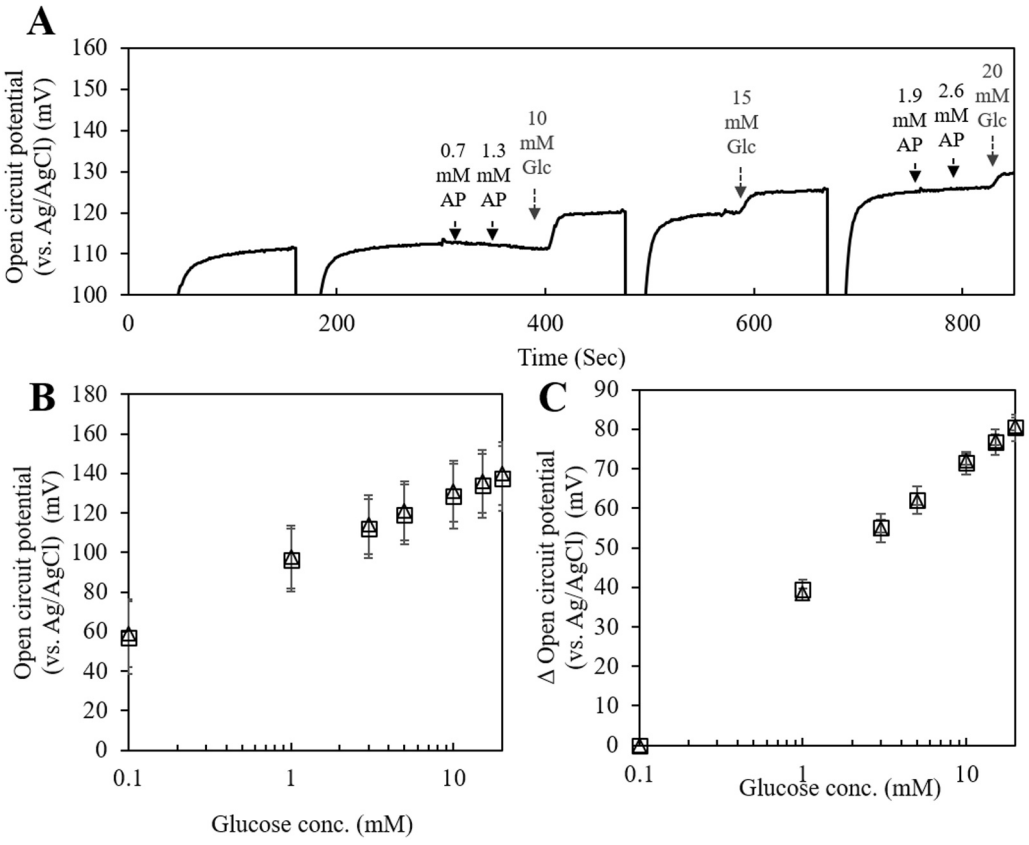

Fig. 4. Investigation of the effect of acetaminophen on the sensor signal of OCP-based third-generation glucose sensor employing a novel measurement algorithm. (A) Representative time course. OCP evaluation of the direct electron transfer FADGDH immobilized electrode in 100 mM potassium phosphate buffer (pH 7.0). Before each OCP data sampling, + 100 mV (vs. Ag/AgCl) was applied to the OCP-based glucose sensor for 10 s. Additionally, we added 0.7, 1.3, 1.9, and 2.6 mM acetaminophen (AP) and 10, 15, and 20 mM glucose at the dashed arrows. We reversed the sign of the potential to ease the interpretation. (B) Comparison of the OCP calibration curve in the absence or presence of 1.3 mM acetaminophen. OCP evaluation of the direct electron transfer FADGDH immobilized electrode in 100 mM potassium phosphate buffer (pH 7.0) in the absence or presence of 1.3 mM acetaminophen. Before each OCP data sampling, + 100 mV (vs. Ag/AgCl) is applied to the OCP-based glucose sensor for 10 s. Open squares show the calibration curve in the absence of acetaminophen, and open triangles show the calibration curve in the presence of 1.3 mM acetaminophen. Evaluations were carried out in triplicate, and error bars indicate the respective standard deviation. We reversed the sign of the potential to ease the interpretation. (C) Comparison of the ΔOCP calibration curve in the absence or presence of 1.3 mM acetaminophen. We calculated the ΔOCP as difference of the OCP value at each glucose concentration to the OCP value in presence of 0.1 mM glucose. OCP evaluation of the direct electron transfer FADGDH immobilized electrode in 100 mM potassium phosphate buffer (pH 7.0) in the absence or presence of 1.3 mM acetaminophen. Before each OCP data sampling, + 100 mV (vs. Ag/AgCl) was applied to the OCP-based glucose sensor for 10 s. Open squares show the calibration curve in the absence of acetaminophen, and open triangles show the calibration curve in the presence of 1.3 mM acetaminophen. Evaluations were carried out in triplicate, and the error bars indicate the respective standard deviations. We reversed the sign of the potential to ease the interpretation.

recommended the investigation of the sensor signal in 1.3 mM acetaminophen. Fig. 4A shows the time course, and we investigated the OCP change by adding acetaminophen and glucose into the reaction buffer. Even with acetaminophen, the OCP was changed only when glucose was added. Additionally, even when 2.6 mM acetaminophen (2 times the FDA-recommended concentration) was added to evaluate the glucose sensor, there was no effect of acetaminophen. Fig. 4B and C shows the calibration curves and slopes of the calibration curves (ΔOCP) with or without 1.3 mM acetaminophen. There was also no significant OCP change in both calibration curves with or without acetaminophen. OCP showed a negative potential in the presence of glucose because the enzyme charged the electrons to the electrode. In the presence of 0.1 mM glucose, the OCP-based glucose sensor showed sufficiently lower potential than the redox potential of these interfering substances. Therefore, these interfering substances cannot affect the electrode surface.

The effect of the presence of Na^+, K^+, or Cl^- on the OCP signal in simulated body fluid (Marques et al., 2011) was also investigated in the physiological concentration range (Gao et al., 2016) and in presence of elevated concentrations (Supplementary information S5). Both OCP and ΔOCP value were decreased slightly due to the increase of ion concentration in the reaction buffer, however, the variation of OCP was within ± 5% which is within the allowed error range for the evaluation of glucose sensor according to the US Food and Drug Administration. The addition of Na^+ (142–242 mM), K^+ (5–55 mM), or Cl^- (149–299 mM) did not cause any significant change of OCP (Supplementary information S6). From this result, it can be considered that the OCP signal is barely affected by a change of ion concentration within the general range of ion concentrations. It was also evident that the performance of the OCP sensor was similar when operated in biological solution or in buffer solution. However, the pH of the solution affected the OCP of electrode itself without affecting the enzyme contribution (Supplementary information S7). Neither the ΔOCP nor the slope of the sensor response were affected by pH. The pH range of interstitial fluid was reported to decrease in some diabetes conditions (Marunaka et al., 2015), however, the OCP signal can be normalized simply by combining a pH sensor. From these data, the OCP-based third-generation glucose sensor employing our novel OCP measurement algorithm can measure only the glucose concentration accurately without being affected by interfering substances such as ascorbic acid, acetaminophen or ion concentrations. Although the OCP is affected by changes in pH, the OCP signal can be normalized simply by combining a pH sensor, because only the background value of OCP is affected by the pH change.

3.3. Continuous measurement of the OCP based on the third-generation glucose sensor employing a novel measurement algorithm

Finally, we investigated the long-term operation of the OCP-based third-generation glucose sensor employing our novel OCP measurement algorithm by continuous OCP measurement in the presence of 20 mM glucose. We carried out calibrations by washing the electrode and changing the reaction buffer and then calculated the slopes of the calibration curves. After 1 h of incubation, OCP signal was stabilized and was ready to monitor. Fig. 5A shows the time course of OCP and slopes of the calibration curves during 9 days. The OCP values observed during the 9 days continuous operation were within ± 10%. Fig. 5B

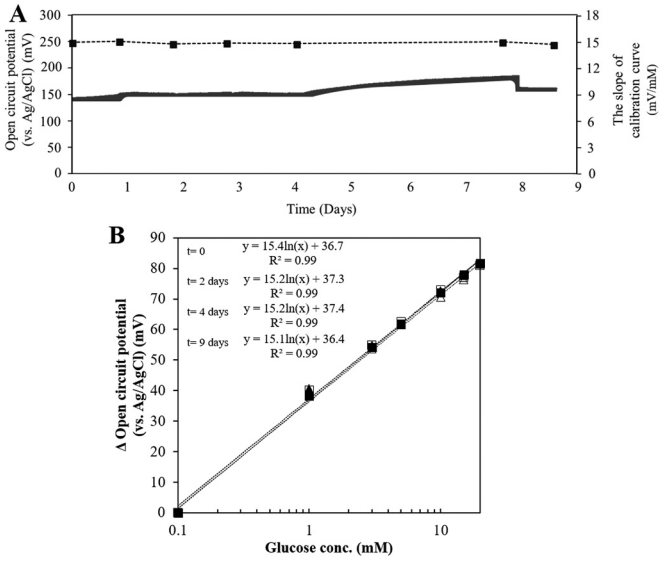

Fig. 5. Continuous measurement of the OCP-based third-generation glucose sensor employing a novel measurement algorithm. (A) OCP evaluation of the direct electron transfer FADGDH immobilized electrode in 100 mM potassium phosphate buffer (pH 7.0) including 20 mM glucose. Before each OCP data sampling, + 100 mV (vs. Ag/AgCl) was applied to the OCP-based glucose sensor for 10 s. We reversed the sign of the potential to ease the interpretation. (B) Representative calibration curve. OCP evaluation of the direct electron transfer FADGDH immobilized electrode in 100 mM potassium phosphate buffer (pH 7.0). Before each OCP data sampling, + 100 mV (vs. Ag/AgCl) was applied to the OCP-based glucose sensor for 10 s. Filled squares show the calibration curve before starting continuous measurement (t = 0), open squares show the calibration curve 2 days after starting continuous measurement (t = 2 days), filled triangles show the calibration curve 4 days after starting continuous measurement (t = 4 days), and open triangles show the calibration curve 9 days after starting continuous measurement (t = 9 days). We reversed the sign of the potential to ease the interpretation.

Table 2
The slopes of calibration curves and the standard deviation of all slopes during continuous measurement. We calculated the normalized slope (%) with 100% being the slope before starting continuous measurement.

Days	The slope of calibration curve (mV/mM)	The normalized slope (%) (100% = the slope before starting continuous measurement)
0	15.4	100.0
1	15.5	100.8
2	15.2	98.9
3	15.3	99.5
4	15.2	99.0
8	15.4	100.2
9	15.1	98.4
Standard deviation (the all slopes during continuous measurement)		0.1

shows the calibration curve before starting continuous measurement and 2 days, 4 days and 9 days after starting continuous measurement, and all the slopes of the calibration curves overlapped perfectly. The slope of the calibration curve 9 days after starting continuous measurement maintained 98% of the slope before starting continuous measurement, and the standard deviation of the slopes were sufficiently low (Table 2). Thus, it was demonstrated that the third-generation OCP-based glucose sensor employing a novel OCP measurement algorithm could measure the glucose concentration stably during 9 days.

In continuous measurements, several reasons can lead to a decrease in sensor stability over time, one of which is enzyme inactivation due to enzyme turnover (Gray et al., 1989). However, with our OCP-based glucose sensor employing a novel OCP measurement algorithm, there were no changes of the calibration curves. It means that enzyme inactivation due to enzyme turnover did not occur during 9 days. As mentioned previously, there is no current in the open circuit state. Accordingly, when the electrode is fully charged, the enzyme can no longer charge electrons to the electrode, and it is considered that enzyme turnover will stop. This characteristic of an open circuit is very suitable to apply for CGM sensors because we can greatly improve long-term sensor stability by minimizing enzyme turnover. Among the current commercially available CGM sensors approved by the FDA, the longest sensor duration is 10 days. On the other hand, although there is no excess quantity of enzyme on the electrode surface because the enzyme was immobilized as a monolayer with SAM, OCP-based third-generation CGM sensor employing our novel OCP measurement algorithm were very stable during 9 days. Due to the advantages of this sensor, we believe that the third-generation OCP sensor based on our novel measurement algorithm will lead to the development of the most highly stable and accurate CGM sensor. Further investigations are still required; however, we expect that we can use this sensor as a CGM sensor that can be used for a long term (over several months) and does not need daily calibration in the future.

4. Conclusion

In this study, we developed an OCP based glucose sensor employing a novel OCP measurement algorithm which will be useful for future CGM application. The third-generation OCP-based glucose sensor employing our novel measurement algorithm showed high reproducibility in measurement and enzyme electrode preparation, and was not affected by interfering substances. Also, the third-generation OCP-based glucose sensor could measure the glucose concentration stably during 9 days without any changes of calibration curves. We believe that the third-generation OCP sensor based on a novel measurement algorithm is very suitable for CGM, and will lead to the development of the most highly stable and accurate CGM sensor.

Acknowledgements

I.L. was financially supported by the Leading Graduate School of Tokyo University of Agriculture and Technology, Japan and Nakatani Foundation for advancement of measuring technologies in biomedical engineering, Japan.

Appendix A. Supporting information

Supplementary data associated with this article can be found in the online version at doi:10.1016/j.bios.2018.09.099

References

Gao, W., Emmaninejad, S., Nyein, H.Y.Y., Challa, S., Chen, K., Peck, A., Fahad, H.M., Ota, H., Shiraki, H., Kiriya, D., Lien, D.H., Brooks, G.A., Davis, R.W., Javey, A., 2016. Nature 529, 509–513.
Gray, M.R., 1989. Biotechnol. Adv. 7, 527–575.
Hanashi, T., Yamazaki, T., Tsugawa, W., Ferri, S., Nakayama, D., Tomiyama, M., Ikebukuro, K., Sode, K., 2009. Biosens. Bioelectron. 24, 1837–1842.
Hanashi, T., Yamazaki, T., Tsugawa, W., Ikebukuro, K., Sode, K., 2011. J. Diabetes Sci. Technol. 5, 1030–1035.
Hanashi, T., Yamazaki, T., Tsugawa, W., Ikebukuro, K., Sode, K., 2012. Electrochemistry 80, 367–370.
Hanashi, T., Yamazaki, T., Tanaka, H., Ikebukuro, K., Tsugawa, W., Sode, K., 2014. Sens. Actuators B: Chem. 196, 429–433.
Inose, K., Fujikawa, M., Yamazaki, T., Kojima, K., Sode, K., 2003. Biochim. Biophys. 1645, 133–138.
Kakehi, N., Yamazaki, T., Tsugawa, W., Sode, K., 2007. Biosens. Bioelectron. 22, 2250–2255.
Katz, E., Buckmann, A.F., Willner, I., 2001. J. Am. Chem. Soc. 123, 10752–10753.
Lee, H., Hong, Y.J., Baik, S., Hyeon, T., Kim, D., 2018. Adv. Healthc. Mater. 7, 1701150.

Lee, I., Sode, T., Loew, N., Tsugawa, W., Lowe, C.R., Sode, K., 2017. Biosens. Bioelectron. 93, 335–339.
Lee, I., Loew, N., Tsugawa, W., Lin, C.E., Probst, D., La Belle, J.T., Sode, K., 2018. Bioelectrochemistry 121, 1–6.
Marques, M.R.C., Loebenberg, R., Almukainzi, M., 2011. Dissolut. Technol. 18, 15–28.
Marunaka, Y., 2015. World J. Diabetes 15, 125–135.
Moatti-Sirat, D., Poitout, V., Thome, V., Gangnerau, M.N., Zhang, Y., Hu, Y., Wilson, G.S., Lemonnier, E., Klein, J.C., Reach, G., 1994. Diabetologia 37, 610–616.
Mori, K., Nakajima, M., Kojima, K., Murakami, K., Ferri, S., Sode, K., 2011. Biotechnol. Lett. 33, 2255–2263.
Ohara, T.J., Rajagopaian, R., Heller, A., 1994. Anal. Chem 66, 2451–2453.
Rodbard, D., 2016. Diabetes Technol. Ther. 18, S2–3-S2-13.
Shiota, M., Yamazaki, T., Yoshimatsu, K., Kojima, K., Tsugawa, W., Ferri, S., Sode, K., 2016. Bioelectrochemistry 112, 178–183.
Sode, K., Tsugawa, W., Yamazaki, T., Watanabe, M., Ogasawara, N., Tanaka, M., 1996. Enzym. Microb. Technol. 19, 82–85.
Sode, K., Yamazaki, T., Lee, I., Hanashi, T., Tsugawa, W., 2016. Biosens. Bioelectron. 76, 20–28.
Song, Y., Su, D., Shen, Y., Liu, H., Wang, L., 2017. Anal. Bioanal. Chem. 409, 161–168.
Tsuya, T., Ferri, S., Fujikawa, M., Yamaoka, H., Sode, K., 2006. J. Biotechnol. 123, 127–136.
Yamaoka, H., Ferri, S., Fujikawa, M., Sode, K., 2004. Biotechnol. Lett. 26, 1757–1761.
Yamashita, Y., Suzuki, N., Hirose, N., Kojima, K., Tsugawa, W., Sode, K., 2018. Int. J. Mol. Sci. 19, 93.
Yamazaki, T., Tsugawa, W., Sode, K., 1999. Biotechnol. Appl. Biochem. 77, 325–335.